

Numerical Modelling of Thermal Distribution Control in a Furnace

¹Petinrin M. O., *^{1,2}Ajide O. O., ¹Dare A. A., ¹Oyewola O. M. and ¹Ismail O.S.

¹Department of Mechanical Engineering, University of Ibadan, Ibadan, Nigeria

²Department of Mechanical Engineering, Howard University, 2300 6th Street NW, Washington, DC, USA, 20059.

*Corresponding author

Email: olusegun.ajide@howard.edu

Alternate email: ooe.ajide@gmail.com

Mobile: 2408987579, +2348062687126

ABSTRACT: Application of control to heat treatment processes helps to achieve the desired mechanical properties of materials but improper controller design is a major problem causing short lifespan of components of locally made furnaces. In this study, the numerical control of the temperature distribution within a furnace cavity was carried out using COMSOL Multiphysics and Simulink. Six sensor points within the furnace cavity (with and without specimen) were selected and each point was consecutively used to observe the time response of the sensor to the desired temperature. The results from the time response analysis indicated uneven temperature distribution within the furnace with points located at the corners of the furnace recording the highest temperature rise while points at the centre of the furnace or within the specimen having the lowest temperature. Thus, the best position for a sensor is at any corner of the furnace to protect the components of the furnace from damage.

KEYWORDS: Thermal controller, sensor, Furnace, Heating element, Heat flux

Date of Submission: 19-07-2018

Date of acceptance: 24-07-2018

I. INTRODUCTION

Heat treatment is highly crucial in manufacturing industry for the development of the state-of-art materials which in turn can influence the quality of machineries production. It has been used as a veritable tool for improving physico-mechanical, thermal and chemical properties of materials. Laudable attempts have been made on works that focuses on the influence of heat treatment on properties of materials.

Daramola et al. [1] carried out investigations to study the effects of heat treatment on the mechanical properties of rolled medium carbon steel. The steel was heated to the austenizing temperature of 830 °C and then water quenched. The obtained results showed that the steel developed has an outstanding improvement in tensile strength, impact strength and ductility which makes it suitable for structural applications. The production of superconducting radio frequency (SRF) cavities is a technology that has already been globally accepted [2]. It was further remarked that, one of the main procedures during the fabrication of SRF cavities is the heat treatment at 600 °C for 10 h or 800 °C for 3 h in ultra-high vacuum (UHV). It was found that heat treatment is required to reduce the mechanical stress in the cavities after fabrication. In the work of Sidhu [3], tremendous yield strength (greater than 1.7 GPa) and good deformability were observed in nanobainitic steel after isothermal heat treatment at a low temperature of 250 °C for a relatively short duration of 24 hours.

Talabi et al. [4] examined the effects of heat treatment processes on the mechanical properties of as-cast Al-4% Ti alloy samples. The outcome of the study showed that as-cast Al-4% Ti alloy produced significant effect on the rigidity and strain characteristics of the alloy. Significant improvement in the ductility of the samples was recorded in the tempered sample. The mechanical properties of Al-Si-Mg cast aluminum alloys such as A356 and A357 used for engine applications do not only depend on casting process, but highly influenced by heat treatment [5]. To understand the influence of microstructural change on mechanical properties of Haynes 282, tensile test was performed at room temperature on the heat treated samples [6]. The gamma prime morphology was observed to change from cuboidal to spherical and then to bimodal in three different heat treatment conditions. The strength of the material is affected by the size and shape of the cuboidal precipitates, while the ductility at room temperature was reasoned to be affected by interconnected morphology of the carbides at the grain boundaries. Super duplex stainless steels were subjected to solution annealing heat treatment at 1050 °C for two hours followed by water quenching in a study carried out by Davanageri [7]. Results obtained showed an improvement in the mechanical and chemical characteristics of the alloys. This was attributed to the formation of secondary phases such as sigma (σ), Chi (χ), secondary austenite (χ_2), carbides, nitrides and intermetallics originating from the cast microstructure which dissolved at high heat treatment temperatures. It was also observed that water quenching assisted enormously in preventing the reoccurrence of precipitation thereby keeping large quantities of solute atoms in solid solution. Tanwer [8] investigated the effect of heat treatment (annealing, normalizing and quenching) on the mechanical properties of stainless steel. Although the three heat treatment techniques adopted in the study showed a general improvement in elongation, the effect of normalizing was found to be most significant. More remarkable efforts have been made on the impact of heat treatment in respect of material properties modification [9-12].

Heat treatment which can be described as the controlled heating and cooling of material in order to deliberately modify or alter its properties is usually carried out in furnaces. Rajan et al. [13] described heat treatment furnace as a heating chamber with a refractory or lagged enclosure. It contains charge and has capacity for retaining heat that is measurable and controllable. There are so many types of furnaces and can be grouped into three which are bath, roller-hearth and strand-type furnaces [14]. The high cost of procuring these furnaces is attracting enormous concern. As part of researchers' efforts, a diesel fired heat-treatment furnace using locally sourced materials has been developed [15]. Tests carried out in order to evaluate the performance of the furnace showed heating rate of 61.24 °C/min to attain a pre-set temperature of 900 °C and a fuel consumption rate less than 1.41 L/h. An attempt was made by Ukoba et al. [16] to develop a heat treatment furnace locally. The developed furnace has a maximum temperature capacity of 880 °C in the heating zone and 21 °C temperature reading at the surface of the external casing after a period of 90 minutes. The furnace was found to heat treat both ferrous, non-ferrous metals and their alloys. 3 kg capacity electric induction furnace with a power rating of 2500 W for heat treatment of ferrous and non-ferrous alloys was developed by Anaidhuno and Mgbemena [17]. The furnace which was made from mild steel sheet was monolithically lined with fire clay refractories and designed to attain a temperature of 1200 °C on the automatic control panel. Performance evaluation showed that the temperature of the furnace was maintained at 1200 °C over a period exceeding 2000 seconds.

There is growing need for control of heat and temperature distributions in heat treatment furnace. This is because heat treatment furnaces are sensitive equipment and slight deviations from normal or designed operating conditions can attract enormous damages. Heat transfer simulation within heating furnaces has been considered to be of great significance for prediction and control of furnace performance [18]. Several other efforts have been made in this respect. A numerical method was used by Türkmen [19] for determination of temperature distribution in the furnace. The results obtained were utilized for optimization of gas circulation in the furnace system under examination. Yang et al. [20] investigated thermal performance of the furnace and heating process of the metal pieces. The furnace was used to heat treat dredging pumps and impellers to obtain the required microstructure and mechanical properties (through stress relief, annealing, hardening and tempering). Simulation provides a useful tool for predicting the temperature evolution within the metal pieces during the heat treatment. The outcome of the study indicated an overall energy balance that can be considered as relatively low energy efficiency of the furnace. To improve energy efficiency, design changes were made with the model. This reduces amount of excess air which in turn also save a lot of energy and thus reduces production cost.

Deprea et al. [21] used a 3D model to investigate the temperature distribution of steel strip that is being annealed and the furnace thermocouple probes. The simple model could predict furnace and strip temperatures. Overall, it has a very short solution time and has been found suitable for rapid simulation of alternative furnace operating conditions. The outcome of the study has potentials for optimizing heat treatment quality, plant throughput and energy consumption. Numerical modelling of heat transfer effects arising during heat treatment of single-crystal nickel-based superalloys used for turbine blades in jet engines has been carried out [22]. Control of thermal characteristics during processing is required in order to avoid incipient melting and to attain

properties suitable for service. The authors employed modelling for prediction of the temporal evolution of the temperature distribution inside the treated component, calculated heat transfer coefficients and analyzed the homogeneity of heat transfer.

Although significant efforts have been made on the application of control to heat treatment processes, controller design is one of the major problems causing short lifespan of furnace components and thus mitigating against its local development. This study focuses on the numerical control of the temperature distribution within a furnace cavity with respect to sensor location. Each of the selected locations was consecutively explored for monitoring the time response of the sensor to the desired temperature. The outcome of this investigation could be found useful in design modifications of furnace cavity.

II. MATHEMATICAL MODELLING

Geometrical Model

In this analysis, two-dimensional representation of a muffle furnace cavity and a specimen was considered with assumption that the heating element was just at the surface of the insulating material. The detailed dimension of the furnace cavity is as given in Fig. 1. It was assumed the furnace cavity was filled with air and the specimen to be heat-treated was a medium carbon steel (MCS) while the material of insulation was the fire brick. The thermo-physical properties of these furnace constituents are as shown in Table 1 [23,24].

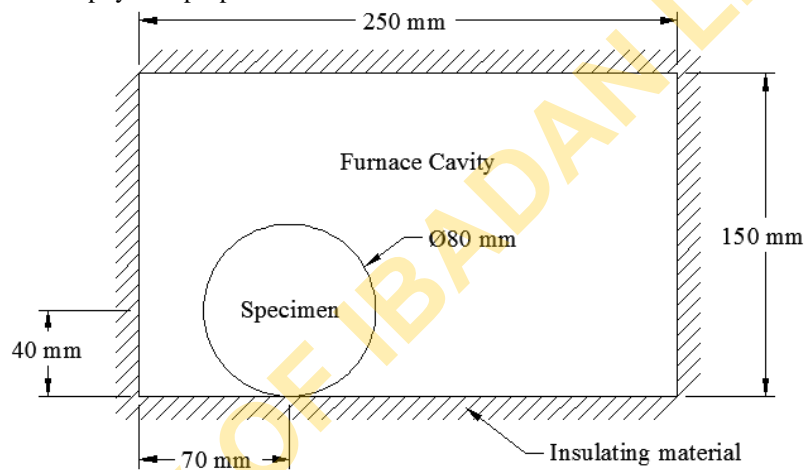


Fig. 1: The dimension of the furnace cavity

Table 1: The Thermo-physical properties of the constituents of the furnace

Properties	MCS	Air	Fire Brick
Density (kg/m ³)	7850	0.6964	-
Thermal Conductivity (W/m ² K)	52.5	0.0407	-
Specific Heat (J/kgK)	485	1030	-
Emissivity	0.12	-	0.75

Modelling of Furnace Cavity without Thermal Controller

In order to simulate transient heat distribution in the furnace, the governing heat equation is given as

$$\rho c_p \frac{\partial T}{\partial t} + \nabla \cdot (-k \nabla T) = 0 \quad (1)$$

where, T is the temperature, k is the thermal conductivity, ρ represents the density, c_p is the specific heat capacity at constant pressure and t is time [23,25]. The initial temperature of the furnace cavity was set to 400 K. Two cases were considered to check the effect of the specimen on the temperature distribution within the furnace, and they are:

- By assuming a constant temperature from the heating element. This can only be achieved if the furnace temperature is under control, therefore the temperature at the wall of the furnace is at a fixed temperature, $T_w = 600$ K
- By taking the power input, P of the heating element to be 4000W, therefore the boundary condition at the furnace wall is set to be

$$-n \cdot (-k \nabla T) = \dot{q} + \varepsilon (G - \sigma T^4) \tag{2}$$

where \dot{q} is the heat flux, ε is the emissivity of material, G is defined to be irradiation on the surface and σ is the Stefan-Boltzmann constant which is $5.670 \times 10^{-8} \text{ W/m}^2\text{K}^4$

The heat flux was determined from the power input and furnace surface area, A as

$$\dot{q} = \frac{P}{A} \tag{3}$$

Also, the irradiation is calculated from

$$G = \frac{J - \varepsilon \sigma T^4}{1 - \varepsilon} \tag{4}$$

And as illustrated in Fig. 2 for radiation exchange between elemental surfaces with elemental areas on each surface, dA_i and dA_j from arbitrarily oriented surfaces A_i and A_j , the radiosity, which accounts for all the rate of radiant energy leaving surface i to surface j is

$$J_i = \frac{q_{i-j}}{A_i F_{ij}} \tag{5}$$

while net rate at which radiation leaves surface i as a result of its interaction with j

$$q_{i-j} = \dot{q} \int dA_i \tag{6}$$

the fraction of the radiation leaving surface i intercepted by surface j known as the view factor is determined from [23,25]

$$F_{ij} = \frac{1}{A_i} \int_{A_i} \int_{A_j} \frac{\cos \theta_i \cos \theta_j}{\pi R^2} dA_i dA_j \tag{7}$$

To ensure heat energy balance between air in the furnace cavity and the specimen, we have

$$-n_a \cdot (-k_a \nabla T_a) - n_s \cdot (-k_s \nabla T_s) = 0 \tag{8}$$

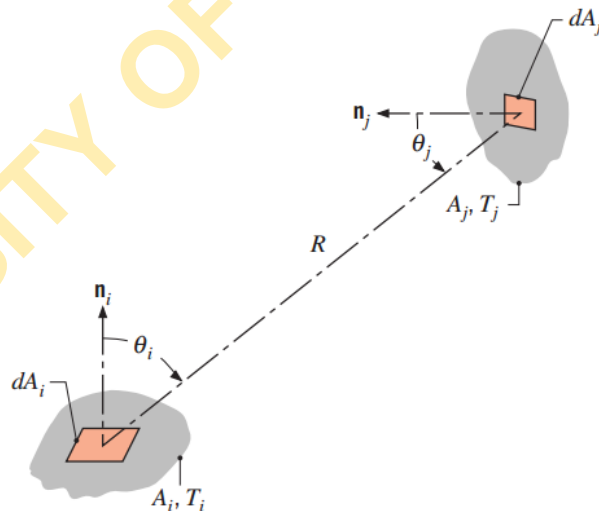


Fig. 2: Radiation exchange between elemental surfaces [23]

The two-dimensional computational domain was discretised using unstructured triangular finite-element meshes. The number of mesh elements are 1047 and 885 for computational model with and without the specimen respectively (Fig. 3). The governing heat equation was solved with a finite element software code, COMSOL Multiphysics using UMFPAK solver for a computational time of 60 s and 2000 s at interval of 0.1 s.

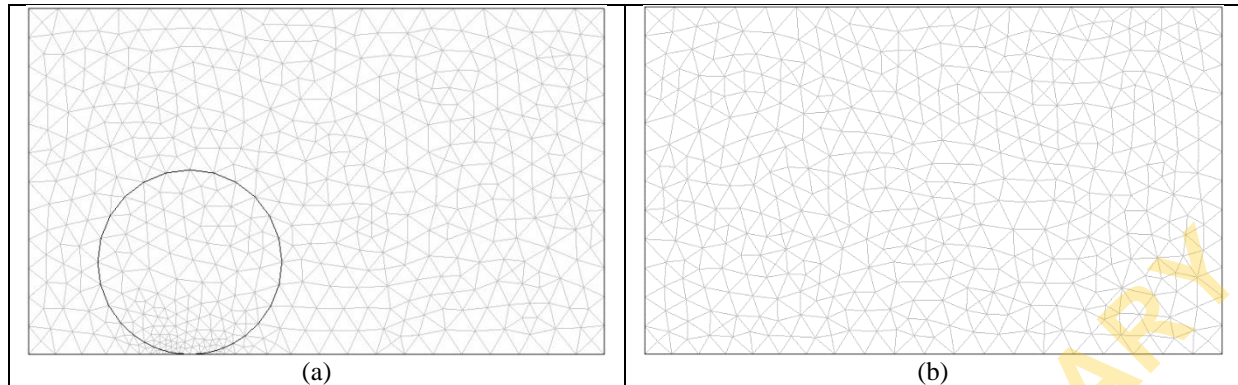


Fig. 3: The finite element discretised model (a) 1047 elements (b) 885 elements

Modelling of Furnace Cavity with Thermal Controller

The time response analysis of the temperature distribution in the furnace under the influence of a thermal controller was carried out in Simulink. With the help of the robust interactive environment of Simulink for non-linear dynamic problems, the complexity that could be involved in completing the simulation in COMSOL Multiphysics was reduced. The location point of the sensor was selected within COMSOL furnace model for every simulation run in Simulink. There were six points selected and each was consecutively used to observe the time response of the sensor to the desired temperature (Fig. 4). With reference to the bottom left-hand corner of the furnace cavity, the points are: PT1 (15 mm, 130 mm), PT2 (15 mm, 20 mm), PT3 (125 mm, 100 mm), PT4 (125 mm, 20 mm), PT5 (235 mm, 130 mm) and PT6 (235 mm, 20 mm). Each model exported from COMSOL to Simulink was implemented as an S-function. This function is solved within Simulink using COMSOL solvers [26].

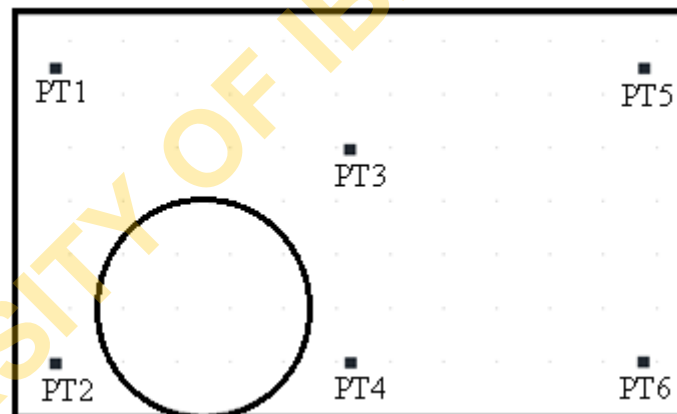


Fig. 4: The probe points for sensor location

The block diagram of the furnace control system is shown in Fig. 5, which includes the furnace, the heating element, an electrical relay, a comparator and a typical thermocouple sensor. Also, the representation of the system in Simulink is as shown in Fig. 6 with the S-function block containing the furnace model being renamed as COMSOL Multiphysics Subsystem. From this figure, the “Flux_State” indicates the state of the heating element, its value is one when the measured temperature, “Temp” is less than the desired temperature but returns zero when the measured temperature is greater than the desired temperature.

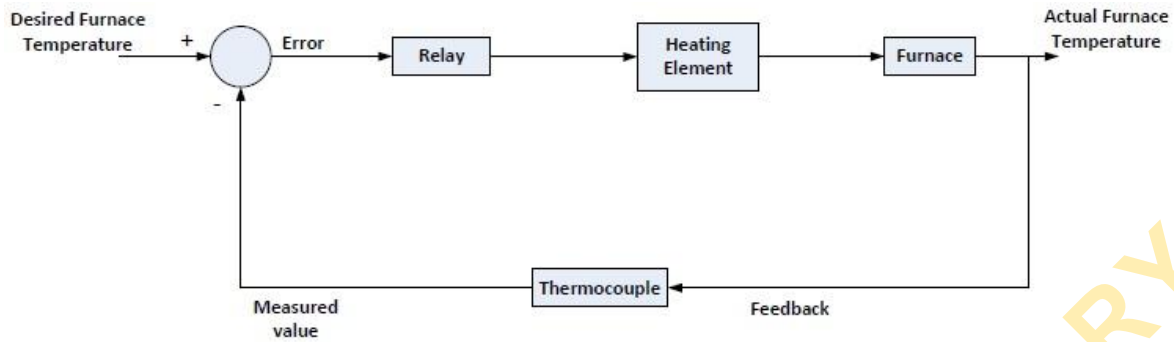


Fig. 5: The block diagram of the furnace control system

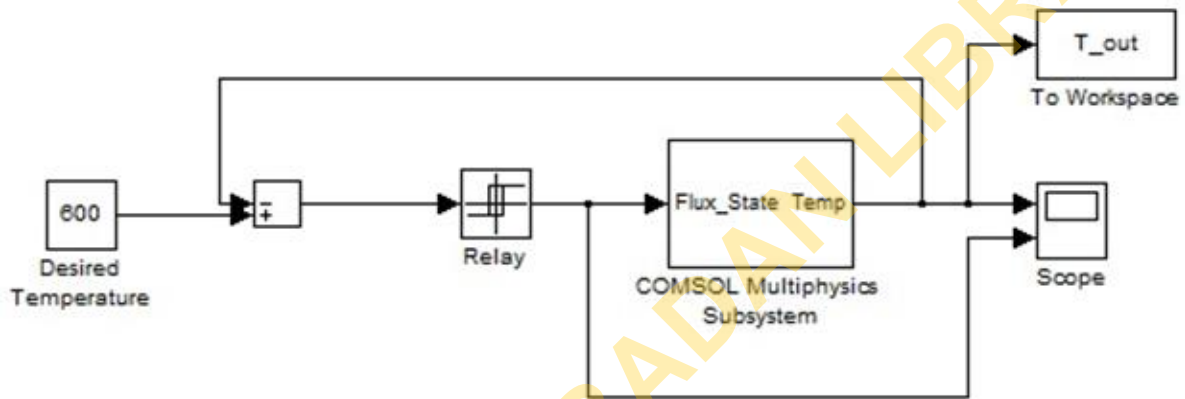
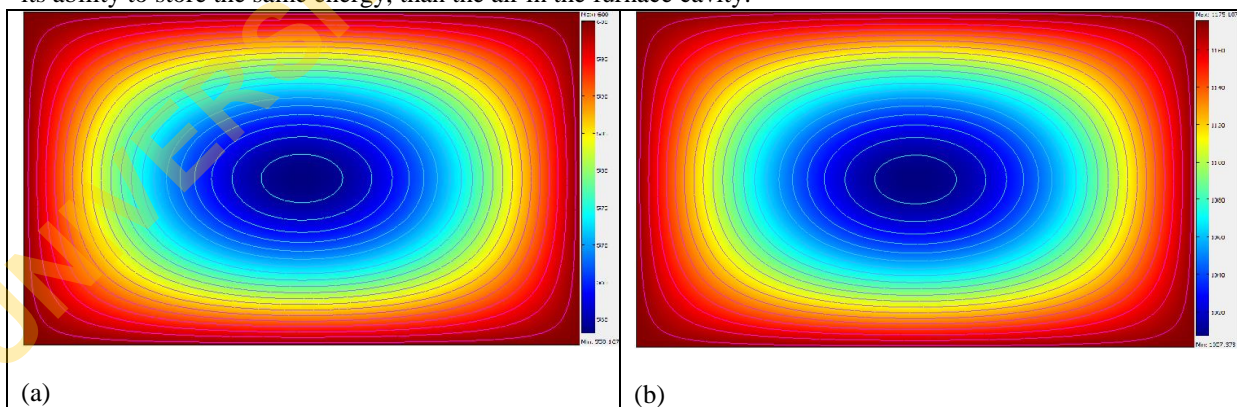


Fig. 6: The furnace control system in Simulink

III. RESULTS AND DISCUSSION

The temperature distributions within the furnace at 60 s are as shown in Fig. 7. From this figure, the minimum and maximum temperatures are 558 K and 600 K; 1007 K and 1175 K; 404 K and 600 K; and 401 K and 1175 K, respectively. Contrary to the distributions of the temperature contours observed in Fig. 7(a) and Fig. 7(b), the lowest temperature points in Fig. 7(c) and Fig. 7(d) were found to be within the specimen. This is because the specimen has lower thermal diffusivity, which is a measure of the ability of a material to conduct heat energy to its ability to store the same energy, than the air in the furnace cavity.



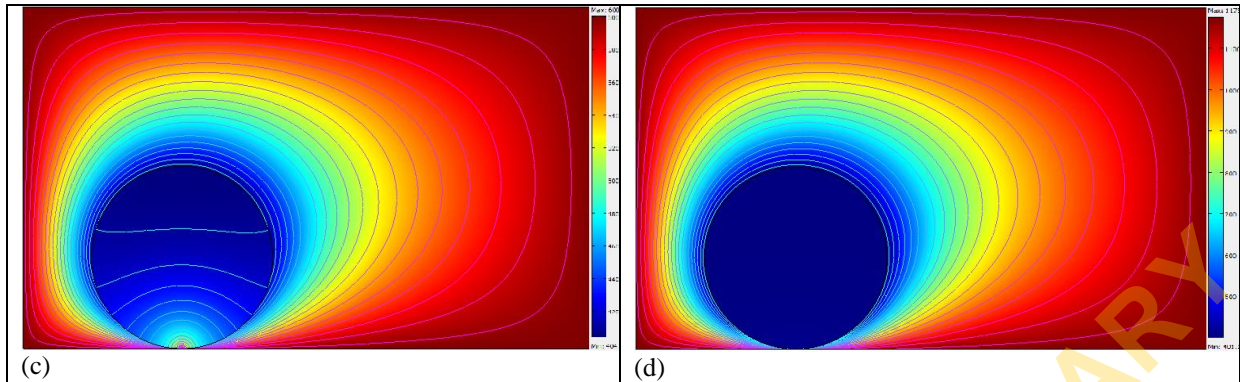


Fig. 7: Temperature contour distribution within the furnace (a) fixed wall temperature without specimen (b) wall heat flux without specimen (c) fixed wall temperature with specimen (d) wall heat flux with specimen.

The plots of temperature rise at the probe points for a period of 60 s in the COMSOL model are shown in Fig. 8 to Fig. 11. The plots for points PT2, PT5 and PT6 were not shown in Fig. 8 and Fig. 9 due to their symmetry with point PT1 without the specimen. Despite the differences in the temperature rise at corresponding points in Fig. 8 to Fig. 11, similar trends were observed in Fig. 8 and Fig. 9, and Fig. 10 and Fig. 11; this is partly because the air convection was assumed to be negligible. Thus, the ratio at which heat is conducted to heat absorption by the air molecules is constant.

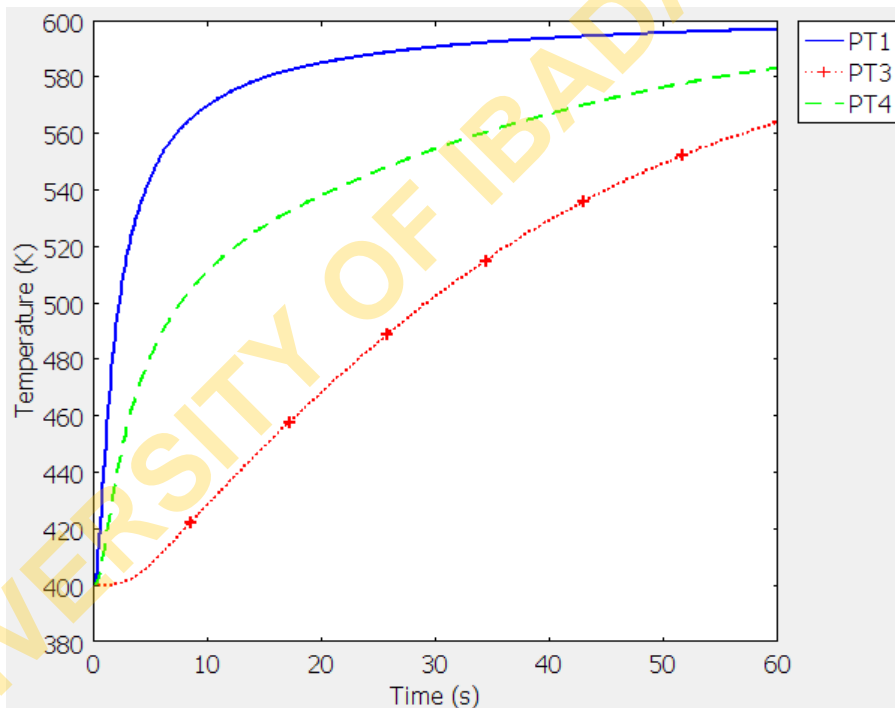


Fig. 8: The rise in temperature at probe points for fixed wall temperature without specimen

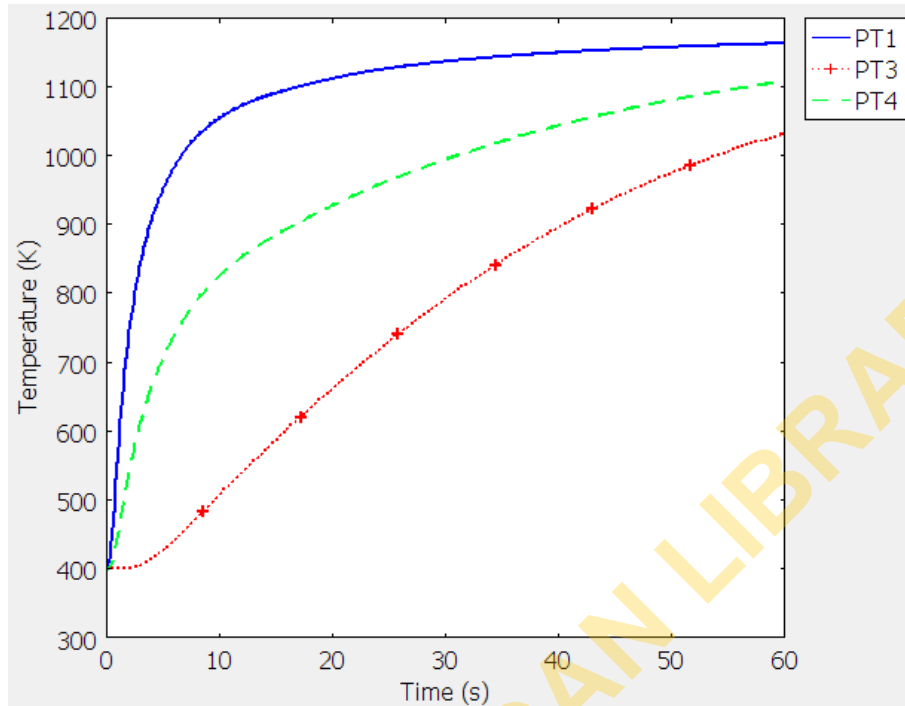


Fig. 9: The rise in temperature at probe points for wall heat flux without specimen

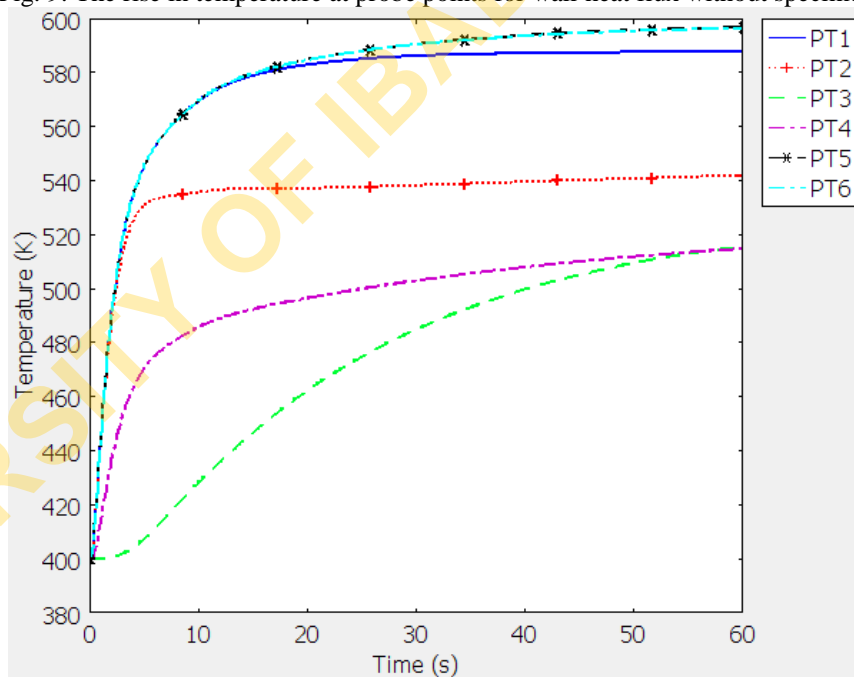


Fig. 10: The rise in temperature at probe points for fixed wall temperature with specimen

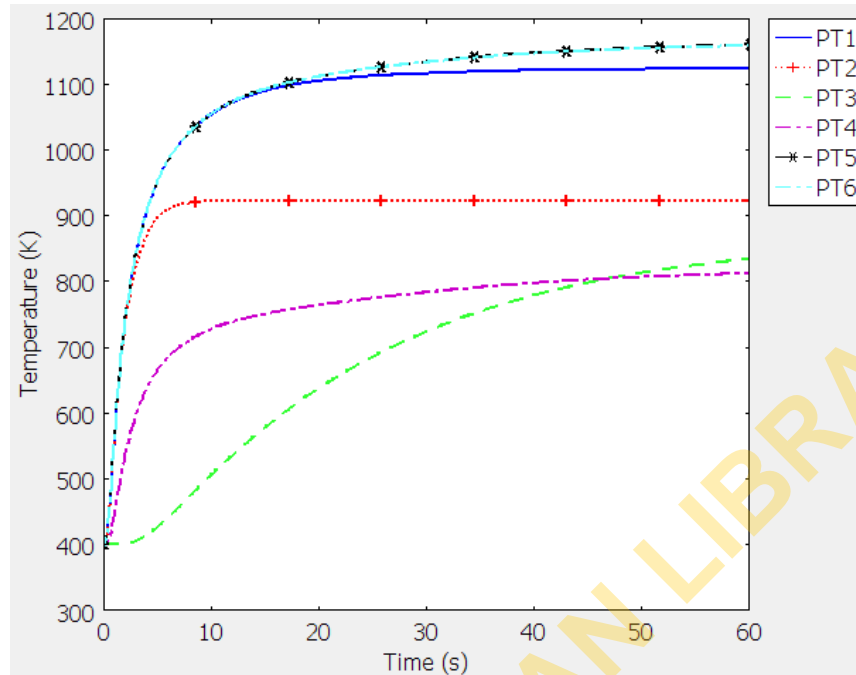


Fig. 11: The rise in temperature at probe points for wall heat flux with specimen

The temperature rises for a period of 2000 s (33 min, 20 s) at all the points when the specimen is within the furnace and fixed furnace wall temperature of 600 K is as shown in Fig. 12. It is obvious from the figure that the temperatures at 2000 s are very close to the wall temperature, and the minimum temperature obtained was found within the specimen at 591 K. This suggests a similar temperature distribution if the furnace heating had been controlled to a temperature of 600 K.

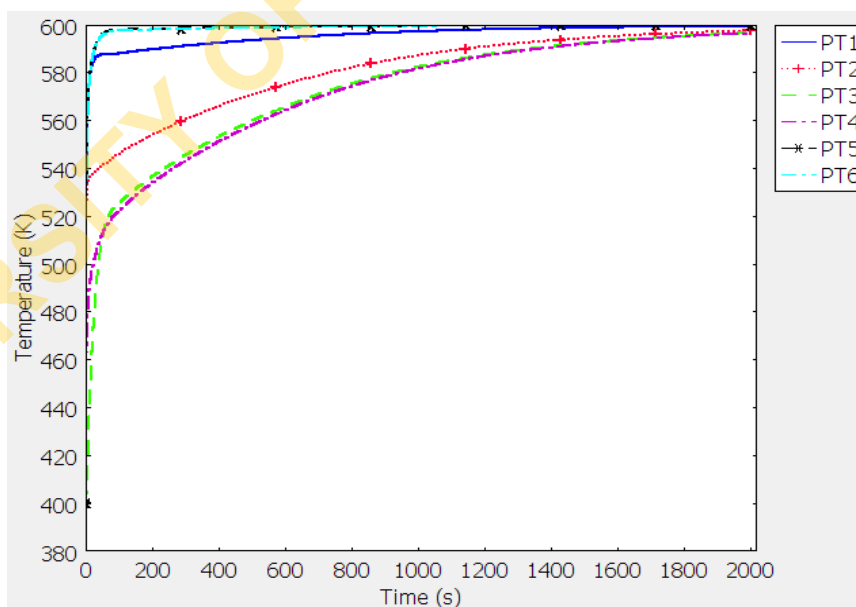


Fig. 12: The rise in temperature within a period of 2000 s for fixed wall temperature with specimen

In the instance of removing the control components in Simulink, the results obtained agreed with the results from COMSOL Multiphysics as indicated in Fig. 13 for PT3 when the furnace cavity with the specimen was subjected to heat flux from heating element. Also, the rise in temperature with the relay output when the heating of the cavity with specimen was under control and the sensor was located at probe point PT3 for 100 s is as depicted in Fig. 14. The relay output indicated one when the desired temperature is below 600 K and

indicated zero when this temperature rises above 600 K. This implies that the heating element would be switched on the output is one and switched off when the output is zero.

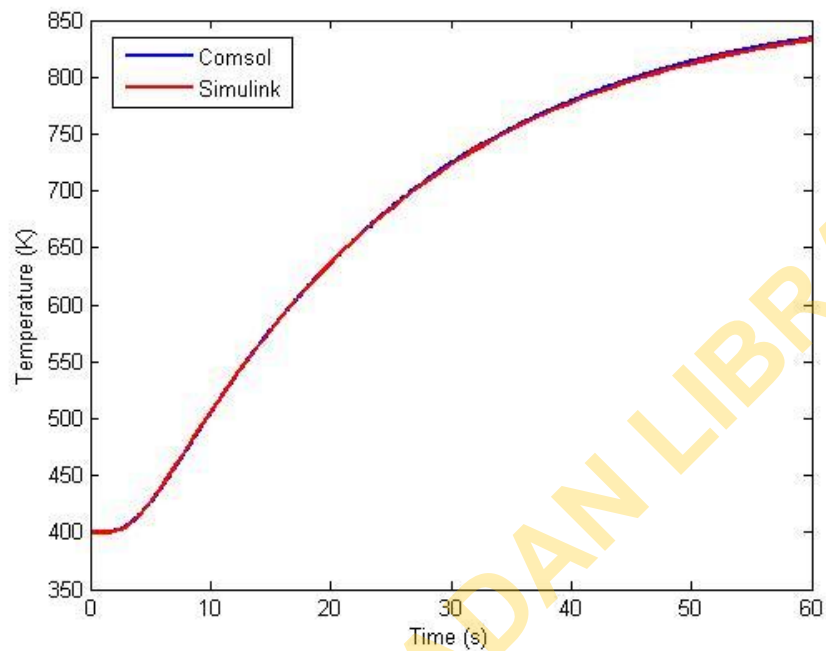


Fig. 13: The rise in temperature at point PT3 in COMSOL Multiphysics and Simulink for wall heat flux with specimen

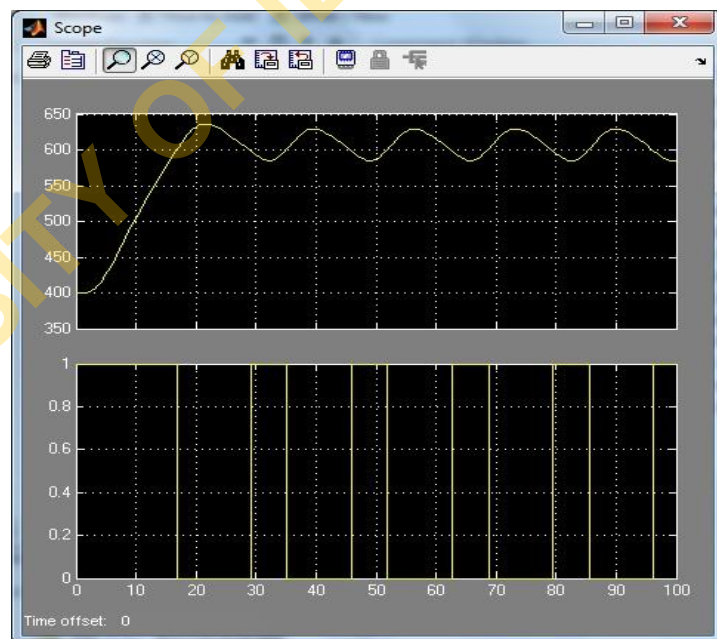


Fig. 14: The controlled temperature distribution and relay output PT3 for wall heat flux with specimen

The time responses at all the probe points, each at a simulation run, when the furnace cavity with the specimen was subjected to heat flux from heating element are as depicted in Fig. 15. Placing the sensor at points PT1, PT2, PT5 and PT6 there were very short rise time with higher overshoot while the longest rise time was recorded at PT3. Hence, to protect the insulating material, heating element, sensor or any other component of the furnace from possible damage, the best position of the sensor is at any corner of the furnace.

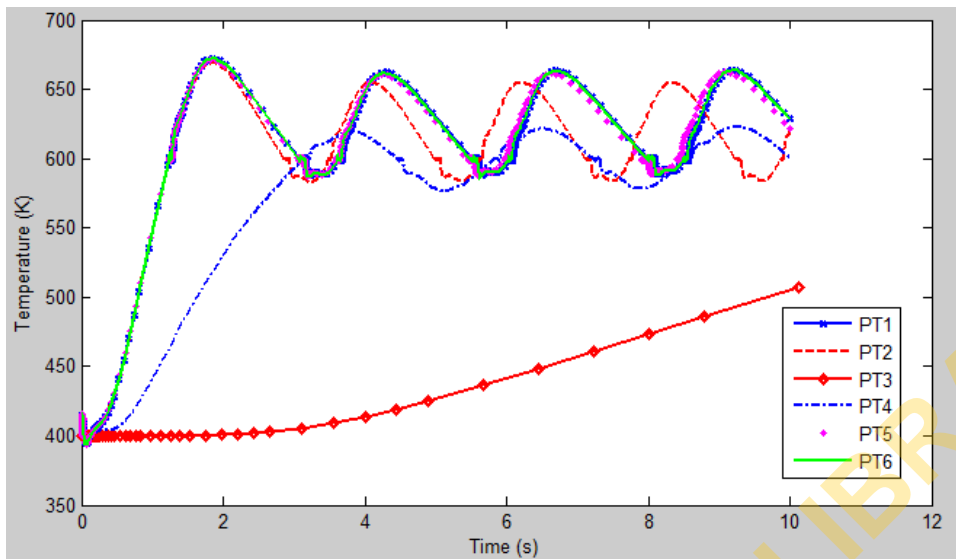


Fig. 15: The controlled temperature distribution at PT3 for wall heat flux with specimen

IV. CONCLUSIONS

The distributed parameter model of a heat-treatment furnace has been simulated successfully with COMSOL Multiphysics and Simulink. The results indicated that spatial temperatures at any particular time are not the same. Sensor positioning at any point close to the wall of the furnace will help to prolong the life span of the heating element, sensor and insulating material.

REFERENCES

- [1] Daramola O.O, Adewuyi B.O., Oladele I.O. (2010). Effect of heat treatment on the mechanical properties of rolled medium carbon steel. *Journal of Minerals & Materials Characterization & Engineering* 9(8):693-708.
- [2] Dhakal P., Ciovati G., Rigby W., Wallace J., Myneni G.R. (2012). Design and performance of a new induction furnace for heat treatment of superconducting radiofrequency niobium cavities. *Review of Scientific Instruments* 83:065105(5 pages).
- [3] Sidhu G. (2013). Modelling and characterization of high carbon nanobainitic steels. Dissertation, Department of Mechanical Engineering, Ryerson University, Toronto, Canada.
- [4] Talabi S.I., Adeosun S.O., Alabi A.F., Aremu I.N., Abdulkareem S. (2013). Effect of heat treatment on the mechanical properties of Al-4%Ti alloy. *International Journal of Metals*, Article ID 127106:1-4.
- [5] Ceschini L., Morri A., Morri A., Rotundo F., Toschi S. (2014). Heat treatment response and influence of overaging on mechanical properties of C355 cast aluminium alloy. *La Metallurgia Italiana* 5:11-17.
- [6] Joseph C. (2015). Microstructural characterization of Haynes 282 after heat treatment and forging. A thesis for the degree of Licentiate of Engineering, Department of Materials and Manufacturing Technology, Chalmers University of Technology, Göteborg, Sweden.
- [7] Davanager M.B., Narendranath S., Kadoli R. (2015). Influence of heat treatment on microstructure, hardness and wear behaviour of super duplex steel AISI 2507. *American Journal of Materials Science* 5(3C):48-52.
- [8] Tanwer A.K. (2014). Effect of various heat treatment process on tensile strength and elongation of stainless steel. *American International Journal of Research in Science, Technology, Engineering & Mathematics* 14-793:195-199.
- [9] Botchararova E., Freudenberger J., Gaganov A., Khlopov K., Schultz L. (2006). Novel Cu-Nb-wires: Processing and Characterization. *Materials Science and Engineering A* 416:261-268.
- [10] Meena A., Mansori M.E. (2012). Material characterization of Austempered Ductile Iron (ADI) produced by a sustainable continuous casting-heat treatment process. *Metallurgical and Materials Transactions A*:1-12.
- [11] Podgornik B., Leskovsek V., Tehovnik F., Burja J. (2015). Vacuum heat treatment optimization for improved load carrying capacity and wear properties of surface engineered hot work tool steel. *Surface & Coatings Technology*, 261: 253-261.
- [12] Santana I.L., Lodovici E., Matos J.R., Medeiros I.S., Miyazaki C.L., Rodrigues-Filho L.E. (2009). Effect of experimental heat treatment on mechanical properties of resin composites. *Braz Deut J.* 20(3): 206-210.
- [13] Rajan T.V., Sharma C.P., Sharma A. (1988). *Heat treatment principles and techniques*, Pergamon press, pp.201-220
- [14] Yudin R.A. (1996). Improving the efficiency of gas-fired heat treatment furnaces. *Metallurgist* 40(7-8):123-129
- [15] Alaneme K.K., Olanrewaju S.O. (2010). Design of a diesel fired heat-treatment furnace. *Journal of Minerals & Materials Characterization & Engineering* 9(7):581-591.
- [16] Ukoba O.K., Anamu U.S., Idowu A.S., Oyegunwa A.O., Adgidzi D., Ricketts R., Olusunle S.O.O. (2012) Development of low heat treatment furnace. *International Journal of Applied Science and technology* 2(7):188-194
- [17] Anaidhuno U.P., Mgbemena C.O. (2015). Development of an electric induction furnace for heat treatment of ferrous and non-ferrous alloys. *American Journal of Engineering Research* 4(5):29-35
- [18] Minea A.A. (2010). Numerical simulation and experimental validation of heat transfer enhancement on a loaded heat treatment furnace. *Journal of Engineering Thermophysics* 19(3):184-191
- [19] Türkman D.A. (2005). Experimental researches of temperature distribution in an electrically heated protective gas tight industrial furnace with gas revolution. *Heat Processing* 3(2):1-5

- [20] Yang Y., Jong R.A., Reuter M.A. (2005). Use of CFD to predict the performance of a heat treatment furnace. Fourth International Conference on CFD in the oil and gas, Metallurgical & Process Industries, SINTEF/NTNU Trondheim, Norway, 6-8 June.
- [21] Depree N., Sneyd J., Taylor S., Taylor M.P., Chen J.J., Wang S., Connor M.O. (2010). Development and validation of models for annealing furnace control from heat transfer fundamentals. Computers and Chemical Engineering 34:1849-1853.
- [22] Consentino F., Warnken N., Gebelin J., Reed R.C. (2013). Numerical modelling of vacuum heat treatment of Nickel-based superalloys. Metallurgical and Materials Transactions A 44A:5154-5164.
- [23] Bergman T.L., Lavine A.S., Incropera F.P., Dewitt D.P. (2011). Fundamentals of heat and mass transfer (7th ed.). John Wiley and Sons, New Jersey.
- [24] GRANTA (2011) CES Edupack. 7.0.0. Granta Design Ltd, Cambridge.
- [25] Naterer G.F. (2003). Heat transfer in single and multiphase systems. CRC Press, Boca Raton.
- [26] Li L., Yang J.J. (2012). Advanced simulation of hydroelectric transient process with Comsol/Simulink. IOP Conference Series: Earth and Environmental Science 12: 1-8.

Petinrin M.O." Numerical modelling of thermal distribution control in a Furnace." American Journal of Engineering Research (AJER), vol. 7, no. 08, 2018, pp. 242-253